

# The AUSGeoid98 geoid model of Australia: data treatment, computations and comparisons with GPS-levelling data

W. E. Featherstone<sup>1</sup>, J. F. Kirby<sup>1</sup>, A. H. W. Kearsley<sup>2</sup>, J. R. Gilliland<sup>3</sup>, G. M. Johnston<sup>4</sup>, J. Steed<sup>4</sup>, R. Forsberg<sup>5</sup>, M. G. Sideris<sup>6</sup>

<sup>1</sup> Department of Spatial Sciences, Curtin University of Technology, GPO Box U1987, Perth, WA 6845, Australia  
e-mail: W.featherstone@curtin.edu.au; Tel.: +61-8-9266-2734; Fax: +61-8-9266-2703

<sup>2</sup> School of Geomatic Engineering, The University of New South Wales, Sydney, NSW 2052, Australia

<sup>3</sup> School of Geoinformatics, Planning & Building, University of South Australia, North Terrace, Adelaide, SA 5000, Australia

<sup>4</sup> Geodesy Section, Australian Surveying and Land Information Group, PO Box 2, Belconnen, ACT 2616, Australia

<sup>5</sup> Geodynamics Department, Kort og Matrikelstyrelsen, Rentermestervej 8, 400 Copenhagen, Denmark

<sup>6</sup> Department of Geomatics Engineering, The University of Calgary, 2500 University Drive NW, Calgary, Alberta T2N 1N4, Canada

Received: 10 March 2000 / Accepted: 21 February 2001

**Abstract.** The AUSGeoid98 gravimetric geoid model of Australia has been computed using data from the EGM96 global geopotential model, the 1996 release of the Australian gravity database, a nationwide digital elevation model, and satellite altimeter-derived marine gravity anomalies. The geoid heights are on a 2 by 2 arc-minute grid with respect to the GRS80 ellipsoid, and residual geoid heights were computed using the 1-D fast Fourier transform technique. This has been adapted to include a deterministically modified kernel over a spherical cap of limited spatial extent in the generalised Stokes scheme. Comparisons of AUSGeoid98 with GPS and Australian Height Datum (AHD) heights across the continent give an RMS agreement of  $\pm 0.364$  m, although this apparently large value is attributed partly to distortions in the AHD.

**Key words:** Practical Geoid Computation – Gravity Data Processing – Modified Kernels – Australia

## 1 Introduction

The determination of the Australian geoid has attracted the attention of geodesists for over three decades. The earliest nationwide geoid model of Australia was computed using astrogeodetic methods (Fisher and Slutsky 1967). At around the same time, nationwide gravimetric geoid models were computed using the gravity data collected during Australia's resource exploration initiatives (Mather 1969; Grushinsky and Sazhina

1971). The Division of National Mapping (NMC), now the Australian Surveying and Land Information Group (AUSLIG), subsequently produced a combined gravimetric-astrogeodetic geoid model of the continent referred to the Australian National Spheroid (Fryer 1972). The NMC recommended this model as the national standard for the reduction of geodetic survey data to this spheroid.

In the mid 1980s, the increasing number of users of GPS in Australia demanded geoid models referred to a geocentric ellipsoid, which prompted further gravimetric geoid computations by Kearsley (1988a, b) and Gilliland (1989). A review of some of the geoid models produced for Australia until 1991 is given in Kearsley and Govind (1992).

In 1991, AUSLIG computed and released a nationwide gravimetric geoid model, called AUSGeoid91, which was referred to the WGS84 ellipsoid. It used the degree-360 expansion of the OSU89A global geopotential model (Rapp and Pavlis 1990), the 1980 release of the Australian Geological Survey Organisation's (AGSO) gravity database, and the ring integration implementation of the spherical Stokes integral (Kearsley 1988a, b) with a limited spherical cap of  $0.5^\circ$  radius.

In 1993, AUSLIG subsequently used the same gravity data and computational procedures based on the degree-360 expansion of the OSU91A global geopotential model (Rapp et al. 1991) to produce a nationwide gravimetric geoid model called AUSGeoid93 (Steed and Holtznagel 1994; Kearsley and Steed 1995). As with the earlier astrogeodetic-gravimetric geoid model, AUSLIG recommended AUSGeoid91 and AUSGeoid93 as the respective national standards for the transformation of GPS-derived ellipsoidal heights to the Australian Height Datum (AHD).

In 1994, the Australian Research Council approved, and thus funded, a University-led project to produce a new generation of gravimetric geoid model for Australia (see e.g. Featherstone et al. 1997b), a description of

which forms the subject of the present paper. The theories, techniques and computer software resulting from this research project were supplied to AUSLIG under licence from Curtin University of Technology. This represents an excellent example of technology transfer from universities to government for the benefit of national geodesy.

In 1998, AUSLIG installed and tested this software on a different computer platform, recomputed a new national gravimetric geoid model following recommendations made by the authors, performed its own verifications and validations (Johnston and Featherstone 1998a, b), and released a product called AUSGeoid98. This supersedes all previous Australian geoid models as the national standard for the transformation of GPS-derived ellipsoidal heights to the AHD.

The use of GPS in conjunction with a geoid model presents a very attractive alternative to conventional spirit levelling in Australia. This is primarily due to the size of the Australian continent, coupled with the relative sparsity of vertical geodetic control provided by the AHD in outback regions. As an example, to transfer vertical geodetic control between two points separated by 50 km takes several days using spirit levelling, whereas it can take only several hours using relative carrier phase GPS in conjunction with a precise geoid model.

In addition, the relatively low order of the spirit-levelling measurements used to establish the AHD has allowed a more ready acceptance of GPS and a geoid model by Australian surveyors as an alternative to spirit levelling. The AHD (Roelse et al. 1971) was established over a few years to support national mapping projects (Lines 1992) using principally third-order spirit levelling. [In Australia, third-order spirit levelling allows a misclose in two-way levelling of  $12\sqrt{d}$  mm, where  $d$  is the distance between points in km (Inter-governmental Committee on Surveying and Mapping, ICSM 1996).] As such, the precision of a geoid model over Australia does not need to be as high as that required in those countries which have higher-order vertical datums to allow the routine use of GPS-based levelling.

This paper gives a self-contained summary of our previously published, and some unpublished, work on several aspects of the Australian gravity field and geoid. Where appropriate, the reader is referred to the cited references for more detailed descriptions of the theories and computational techniques used. Importantly, several of the approaches used for AUSGeoid98 are different to those documented for and adopted in other parts of the world. This is most probably due to the various peculiarities of the Australian data. Nevertheless, these experiences may shed some light on the practical solution of similar problems in other regional gravimetric geoid computations around the world.

All aspects involved in the practical computation and evaluation of AUSGeoid98 are described in three parts. The first part deals with the preparation of the data, since it is important to note that a considerable amount of time and effort are associated with this stage of any continent-wide gravimetric geoid computation. The

second part of the paper deals with the computation of residual geoid undulations using a deterministically modified Stokes kernel over a limited spherical cap in the 1-D fast Fourier transform (1-D-FFT) technique. Finally, results of the fit of AUSGeoid98 to GPS and third-order, or better, spirit-levelled heights on the AHD are used to illustrate the improvements made over AUSGeoid93. These comparisons are also used to identify the *possible* presence of systematic errors in the AHD.

## 2 Data compilation

### 2.1 The EGM96 global geopotential model

EGM96 (Lemoine et al. 1998) was used, complete to spherical harmonic degree and order 360, in a variant of the so-called remove–compute–restore approach. For AUSGeoid98, this expansion of EGM96 was used in conjunction with a low-degree, deterministically modified, spheroidal Stokes kernel, which is theoretically quite distinct from using the (unmodified) spherical Stokes kernel. The spheroidal Stokes kernel is implicit to the generalised Stokes scheme (Vaniček and Sjöberg 1991), which satisfies its own geodetic boundary-value problem (Martinec and Vaniček 1997). The medium- and high-degree components of EGM96 were used in a remove–compute–restore stage based on the higher-than-second-degree reference spheroid in the generalised Stokes scheme. This ‘hybrid approach’ used for AUSGeoid98 will be described in more detail in Sect. 4.

The EGM96 global geopotential model was chosen simply because it was the most recent model available at the time AUSGeoid98 was computed. It includes more data than in other models and uses arguably improved computational techniques. EGM96 and several other global geopotential models have been compared with Australian gravity data and with nationwide GPS and AHD heights (Kirby et al. 1998). EGM96 appears to give a slightly better representation of the gravity field over Australia, although the improvements made over previous global geopotential models are not statistically significant when considering the errors in the Australian data (Sects. 2.2 and 2.5).

### 2.2 Terrestrial gravity data

The 1996 data release of AGSO’s national gravity database (Fig. 1) was used for the computation of AUSGeoid98. This database comprises 696 916 gravity observations on land and 134 539 ship-track observations offshore Australia, which is an increase of over 100 000 observations on the 1980 data release used in AUSGeoid91 and AUSGeoid93. However, this increase has only improved the spatial density of the gravity data coverage in specific areas, since the whole continent was reconnaissance gravity surveyed at an approximate 7–11-km spatial resolution as part of Australia’s resource exploration initiatives (Fraser et al. 1976; Gilliland 1987).

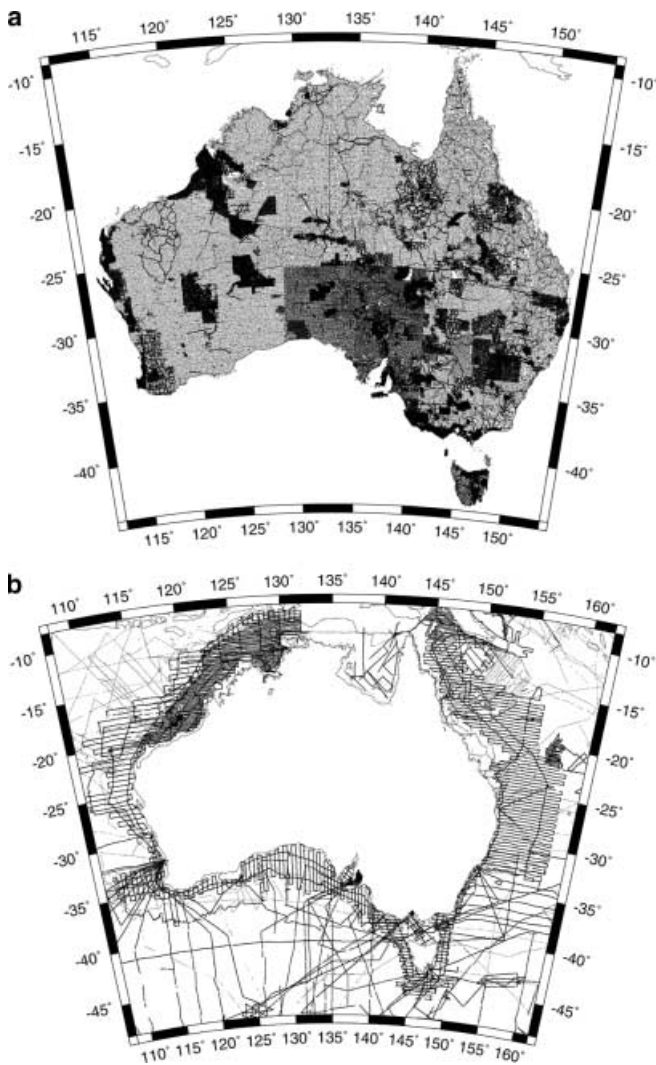


**Fig. 1.** Coverage of the 1996 release of the AGSO gravity database **a** over land and **b** in marine areas (Lambert conical projection)

For the Australian reconnaissance gravity data, the observation errors have been estimated to be  $\pm 0.3$  mGal, with a  $\pm 4$ – $6$  m error in the barometrically determined elevations (see e.g. Featherstone et al. 1997a). Assuming independence and zero error in the topographic mass density, these estimates infer an error in the computed free-air gravity anomaly of  $\pm 1.2$ – $1.8$  mGal, and an error in the simple Bouguer gravity anomaly of  $\pm 2.0$ – $3.0$  mGal.

The datum for all Australian gravity measurements is the IsoGal84 network of base stations (Wellman et al. 1985), which in turn is tied to the International Gravity Standardisation Network 1971 (Morelli et al. 1971). It is not known which variant of tidal correction was applied to the gravity observations by the AGSO, thus the tidal system of AUSGeoid98 remains uncertain. Also, the elevations of the AGSO gravity observations are of variable quality. Part of the reconnaissance gravity survey of Australia was conducted before the establishment of the AHD in 1971. During this survey, the gravimeter and barometer drift were controlled by observing in a ‘clover leaf’ pattern (Fraser et al. 1976), and

the elevations were tied to spirit-levelling traverses, where available. Subsequent gravity surveys have normally been tied to monumented stations of this reconnaissance gravity survey. More recently, GPS and unspecified geoid models have been used to coordinate gravity surveys. Therefore, much of the Australian gravity data is not rigorously tied to the AHD, which affects the accuracy and consistency of the computed gravity anomalies.

Finally, it is assumed that there have been no temporal changes in gravity or elevation in Australia over the approximate 40-year period that the gravity and elevation measurements have been made, so the computed geoid applies to a single epoch.

### 2.3 The Australian digital elevation model

The computations of AUSGeoid91 and AUSGeoid93 omitted some topographic corrections (i.e. gravimetric terrain corrections and their associated indirect effects) because no nationwide digital elevation model (DEM) was available at the time that these geoid models were computed. As such, they are strictly defined as free-air co-geoids, which partly explains why these models have been found to be deficient in areas of rugged terrain (Sect. 5.4). Another reason for this finding may result from the use of unrepresentative mean free-air gravity anomalies in the computation of AUSGeoid91 and AUSGeoid93 (Sect. 3.2). To attempt to numerically counter both of the above effects, the nationwide DEM, supplied by AUSLIG as a 9 by 9 arc-second grid (approximately 250 m) of mean elevations, was used in the computation of AUSGeoid98. The improvements in AUSGeoid98 over AUSGeoid93 made by including topographic information will be shown in Sect. 5.4.

The DEM has been constructed from approximately 5.1 million spot heights held by AUSLIG, approximately 200 000 of the elevations held in the AGSO gravity database, some airborne altimetry profiles and other data (Carroll and Morse 1996). These elevation data have been gridded using a drainage-enforcing algorithm (Hutchinson 1989). The precision of the resulting mean heights in the DEM is estimated to be  $\pm 7.5$  m (Carroll and Morse 1996). The descriptive statistics of the DEM heights on land are (Kirby and Featherstone 1999) as follows: maximum 2193 m; minimum  $-24$  m; mean 134 m; standard deviation  $\pm 190$  m. These values indicate that the topography of the Australian continent is relatively smooth (the highest mountain in Australia is only 2228 m in AHD height). This DEM was used in AUSGeoid98 to compute gravimetric terrain corrections, primary and secondary indirect effects, and to construct mean gravity anomalies on land (Sects. 3.1 and 3.2).

### 2.4 Satellite altimeter-derived marine gravity anomalies

Marine gravity anomalies, derived from satellite-borne radar altimeter measurements, were used offshore

Australia to supplement AGSO's marine gravity data coverage (Fig. 1b). The inclusion of these data significantly improves the spatial density and coverage of gravity data offshore Australia, and thus could be expected to give an improved gravimetric geoid solution in areas on land that are close to the coast. However, this appeared not to be the case from comparisons of preliminary geoid models with GPS and AHD data close to the Australian coast. Therefore, as a practical solution, least squares collocation was used to combine the altimeter and AGSO gravity data (Sect. 3.3).

The satellite altimeter-derived gravity anomalies (assumed to be free-air) were downloaded from the FTP site of the Scripps Institute for Oceanography, California. These gravity anomalies had been computed on a 2 by 2 arc-minute grid from a combination of Geosat, TOPEX/Poseidon and ERS-1 satellite altimeter missions (Sandwell and Smith 1997). It is acknowledged that other sources of altimeter-derived gravity anomalies do exist, such as those at Kort og Matrikelstyrelsen (KMS) in Denmark (see e.g. Knudsen and Andersen 1998). However, the Scripps data were used because they are in the public domain and were readily available at the time that this phase of the AUSGeoid98 project was being undertaken.

### 2.5 GPS and spirit-levelled AHD height data

Geodetic GPS networks that are co-located with orthometric heights provide discrete, geometrical *estimates* of geoid heights with respect to the reference ellipsoid. Strictly speaking, this yields the separation between the local vertical datum and the reference ellipsoid (see e.g. Featherstone 1998). At present, however, these provide the only data available for the practical verification of gravimetric geoid models on land. GPS and orthometric height data can be used in both an absolute and a relative sense to indicate the precision of a gravimetric geoid solution.

- (1) In absolute verifications, the GPS network must have been previously tied to a geocentric, international terrestrial reference frame so as to assess the precision and accuracy of the gravimetric geoid model with respect to a geocentric reference ellipsoid. These data can also be used to apply constraints on the zero-degree term in order to account for the inexact knowledge of the mass of the Earth and potential of the geoid (Heiskanen and Moritz 1967; Sect. 5.2 of the present paper).
- (2) Alternatively, the GPS and orthometric height data can be used in a relative sense to assess the precision of the gravimetric geoid gradients. This relative verification is more representative of the way in which a gravimetric geoid model is used in Australia to transform GPS-derived ellipsoidal height differences to AHD height differences (cf. Kearsley 1998a, b).

It is essential to point out that both of the above verifications of gravimetric geoid models are inevitably subject to errors in the GPS and levelling data, as well as

the practical realisation of the local vertical datum, all of which will be discussed throughout this paper.

The GPS data used for this study come from a variety of geodetic networks across Australia (Fig. 4). These GPS networks are tied to the ITRF92 (epoch 94.0) reference frame as part of the implementation of the Geocentric Datum of Australia. One error estimate for these GPS-derived ellipsoidal heights is  $\pm 50$  mm (e.g. Stewart 1998), but this estimate will increase for the in-fill networks that are constrained to the national GPS networks and for older GPS data held by AUSLIG.

In terms of gravimetric geoid validation in Australia, the accuracy of the levelling data and definition and realisation of the AHD are more problematic. The AHD uses a normal orthometric height system, and the least squares adjustment used heights fixed to zero at 30 tide gauges around the Australian mainland (Roelse et al. 1971) and two tide gauges in Tasmania (National Mapping Council 1986). This, as well as spirit-levelling errors (Sect. 1) and the neglect of observed gravity in orthometric corrections, cause the AHD to depart from a single equipotential surface by approximately 1 m (see e.g. Featherstone 1998).

The AHD was established over a few years using 97 230 km of two-way, third-order (ICSM 1996) spirit-levelling observations, which is considerably less precise than the levelling observations used to validate gravimetric geoid models in some other parts of the world. Therefore, while absolute and relative validations of Australian gravimetric geoid models with GPS and AHD data (Sect. 5) are useful, they cannot be relied upon as an unequivocal vindication of gravimetric geoid determination techniques on land.

## 3 Gravity data processing

### 3.1 Computation of gravimetric terrain corrections and indirect effects

AUSGeoid98, unlike all its gravimetric predecessors, includes gravimetric terrain corrections and primary and secondary indirect effects, which have been computed using the Australian DEM (Sect. 2.3). Mean, terrain-corrected, free-air gravity anomalies, termed mean Faye gravity anomalies (see e.g. Heiskanen and Moritz 1967), were used to approximate mean Helmert gravity anomalies at the geoid for the simple reason of computational convenience (Sect. 3.3).

It is acknowledged that theoretically more rigorous approaches do exist for the computation and downward continuation of mean Helmert gravity anomalies (see e.g. Martinec and Vaniček 1994b; Vaniček and Martinec 1994; Vaniček et al. 1999). However, the Moritz–Pellinen approximation (Moritz 1968) was employed because it is particularly suited to evaluation by FFT techniques (see e.g. Schwarz et al. 1990). The FFT offers a very practical way to compute detailed terrain corrections on a continent-wide scale, since quadrature-based numerical integration could take (an estimated) few months for the Australian DEM.

The Moritz (1968) gravimetric terrain correction ( $C$ ) is given by

$$C = \frac{G\rho R^2}{2} \int_{\sigma} \frac{(H' - H)^2}{l_0^3} d\sigma \quad (1)$$

where  $G$  is the Newtonian gravitational constant,  $\rho$  is the topographic mass density (assumed to be a constant value of  $2670 \text{ kg m}^{-3}$  in AUSGeoid98),  $R$  is the mean radius of a spherical Earth,  $H$  is the elevation of the computation point,  $H'$  is the elevation of each remote point in the integral,  $l_0$  is their planar separation, and  $d\sigma$  is the integration element on the sphere.

The planar, 2-D-FFT expression of Eq. (1) is (Schwarz et al. 1990; Kirby and Featherstone 1999)

$$C = \frac{G\rho R^2}{2} \left( \mathbf{F}^{-1} \left[ \left\{ \sum \mathbf{F}\{1/l_0^3\} \mathbf{F}\{H'^2\} \right\} \right] - 2\mathbf{H}\mathbf{F}^{-1} \left[ \left\{ \sum \mathbf{F}\{1/l_0^3\} \mathbf{F}\{H'\} \right\} \right] \dots + H^2 \mathbf{F}^{-1} \left[ \left\{ \sum \mathbf{F}\{1/l_0^3\} \mathbf{F}\{1\} \right\} \right] \right) \quad (2)$$

where  $\mathbf{F}$  and  $\mathbf{F}^{-1}$  are the 2-D Fourier transform operator and its inverse, respectively. The practical argument against the computation of Helmert gravity anomalies at present in Australia is that the kernel is not readily adaptable to 2-D-FFT implementation, because it is neither homogeneous nor isotropic, and thus has to rely on the time-consuming quadrature-based numerical integration.

The above arguments also apply to the evaluation of the primary indirect effect on the geoid, where theoretically more appropriate formulae relating to the use of Helmert gravity anomalies are also available (see e.g. Martinec and Vaníček 1994a). Again for computational convenience and, moreover, to maintain consistency with the use of Moritz's formula [Eq. (1)], the primary indirect effect on the geoid ( $N_i$ ) was computed using the quadratic term of Wichiencharoen's (1982) formula

$$N_i = -\frac{\pi G\rho H^2}{\gamma} \quad (3)$$

where  $\gamma$  is normal gravity on the surface of the reference ellipsoid. The higher-order terms in Moritz's (1968) and Wichiencharoen's (1982) formulae were not considered. However, future experiments will be used to estimate the significance of the errors associated with the approximations in Eqs. (1) and (3), as well as applying the Helmert technique, to Australia.

Kirby and Featherstone (1999) describe the computation of the gravimetric terrain corrections over Australia using the 2-D-FFT and the linear term of Moritz's formula [Eq. (2)]. However, there are some pertinent points that are worth summarising here. Due to computer memory restrictions at the time, the terrain correction computations were conducted in a series of  $1.5^\circ$ -wide overlapping longitudinal bands. The integration radius was chosen to be 50 km, which was imple-

mented in the 2-D-FFT by setting the kernel to zero outside this radius before Fourier transformation to the frequency domain (cf. Sect. 4.2). It is acknowledged that this truncated integration omits long-wavelength contributions of the terrain correction, which are systematically positive. Therefore, further work is required to investigate the significance of this issue to geoid computations in Australia.

It is noted that the approximations implicit to Moritz's (1968) approach [Eq. (1)] cause it to become unstable for very dense DEM grids (Martinec et al. 1996). This appeared to be the case in Australia, where the use of the 9 by 9 arc-second DEM revealed over 60 'spikes' in the computed terrain corrections of greater than 100 mGal (maximum: 273.63 mGal). These are very unlikely to be correct values in the relatively smooth Australian topography (see Sect. 2.3). Kirby and Featherstone (1999) attributed these spikes to the instability in the Moritz algorithm.

However, such problems have not been reported in other parts of the world when using DEMs of a higher spatial resolution, such as in Scandinavia and the USA. Subsequent investigations confirm the presence of gross errors in the Australian DEM, where terrain gradients of greater than  $70^\circ$  are implied by the DEM. Moreover, these are spatially correlated with the spikes found in the 9 by 9 arc-second terrain corrections. In retrospect, it would have been preferable to clean the DEM, but unfortunately these errors were not detected at the time. AUSLIG are currently computing a new DEM.

A parallel consideration is the accuracy of the DEM data used to compute the terrain corrections. Zhang (1997) shows that the  $\pm 7.5$  m error associated with the 9 by 9 arc-second DEM (Carroll and Morse 1996) can cause errors of greater than 100% in the computed terrain corrections in some (generally low-lying) areas. In order to avoid this and the spikes in the terrain corrections, a coarser DEM grid was used, where the 9 by 9 arc-second DEM was generalised onto a 27 by 27 arc-second grid, assuming that – with no correlations – the error in the DEM heights is decreased.

Therefore, the gravimetric terrain corrections used in AUSGeoid98 were computed on a 27 by 27 arc-second grid (approximately 750 m) over the Australian continent. The descriptive statistics of these terrain corrections are as follows (Kirby and Featherstone 1999): maximum 40.34 mGal; minimum 0 mGal; mean 0.07 mGal; standard deviation  $\pm 0.40$  mGal. The use of a 27 by 27 arc-second grid spacing omits the high-frequency terrain corrections and near-meter effects. Also, the integration radius of 50 km omits some of the long-wavelength terrain corrections. Accordingly, AUSGeoid98 has used bandwidth-limited terrain corrections.

The primary indirect effect [Eq. (3)] was also computed from the 27 by 27 arc-second DEM grid, which is consistent with the use of the linear term of Moritz's formula and the DEM grid-spacing in the terrain correction computations. It is useful to note that, from a practical point of view, the primary indirect effect should be evaluated prior to the computation of the geoid

because it allows the computation of the secondary indirect effect on gravity. This then allows the geoid to be computed in a single stage, rather than separately computing the geoid signal from the secondary indirect effect. This secondary indirect effect was computed for AUSGeoid98 by applying the linear free-air reduction over the geoid/co-geoid separation estimated by the primary indirect effect (i.e.  $0.3086 N_i$  [m] mGal). This resulted in an additional gravity term that was generalised from the 27 by 27 arc-second grid to a 2 by 2 arc-minute grid, then added to the grid of mean Faye gravity anomalies (described next).

### 3.2 Computation of mean Faye gravity anomalies

As the AGSO terrestrial gravity data (Sect. 2.2) were collected and reduced predominantly for geophysical exploration purposes, they are not necessarily suited to the requirements of gravimetric geoid computation. As such, they have been verified according to the procedures described in Featherstone et al. (1997a) and point gravity anomalies computed using the more stringent geodetic approaches. Point simple Bouguer gravity anomalies were calculated from the observed data using a second-order free-air reduction (see e.g. Featherstone 1995), normal gravity at the surface of the GRS80 ellipsoid via the Somigliana–Pizetti formula (Moritz 1980), an atmospheric correction developed from a second-order polynomial fit to the IAG tables (Featherstone et al. 1997a), and a constant topographic mass density of  $\rho = 2670 \text{ kg m}^{-3}$ .

While the latter value is a common choice for this parameter, it is a gross oversimplification for the Australian continent, which possesses many geological terranes with topographic mass densities contrasting by up to  $1000 \text{ kg m}^{-3}$  (see e.g. Featherstone 2000). However, detailed topographic density information is not available for the whole Australian continent, hence the choice of this standard value. The use of a constant topographic mass density will cause an error in all of the computed simple Bouguer gravity anomalies, gravimetric terrain corrections and indirect effects.

The numerical solution of the Stokes integral, or a modification thereof, using the 1-D-FFT technique (Haagmans et al. 1993) requires a complete and regular grid of mean gravity anomalies. This is to ensure that the numerical integration mimics analytical integration as closely as possible. On land, the point simple Bouguer gravity anomalies were interpolated from their observed positions using continuous-curvature splines in tension (Smith and Wessel 1990) to produce a 9 by 9 arc-second grid. Other gravity gridding techniques do exist, such as least squares collocation, but the tensioned-spline algorithm was readily available and gives very similar results in a considerably shorter time (Zhang 1997).

It is acknowledged that simple Bouguer gravity anomalies are not necessarily best suited to gravity data gridding. This is because terrain corrections remove some of the high-frequency information from the simple Bouguer gravity anomalies, thus making them less

subject to aliasing during the gridding process. However, experiments with the Australian gravity data (Zhang 1997) used free-air, complete Bouguer and topographic–isostatic gravity anomalies (with a constant topographic mass density) to predict gravity anomalies at independent points where gravity had been observed (i.e. these points were not used in the gridding). Comparison of the predicted and observed gravity anomalies showed that not one of the anomaly types is consistently the best suited to gravity data gridding in Australia. Therefore, the question of aliasing during gridding because of the type of gravity anomaly used remains open.

Many of the Australian land gravity observations were made along roads and tracks in areas of rugged terrain, which usually follow valleys or areas of least height variation. A similar, though opposite, effect occurs in outback Australia, where most observations were collected using helicopter transport (Fraser et al. 1976). These observations were often located on raised ground where convenient helicopter landing spots were identified. As such, any mean gravity anomalies computed from only these point observations, and any subsequently determined geoid, will be biased due these data acquisition strategies.

The consequences of this improper sampling of the Australian gravity field are twofold. First, the mean free-air gravity anomalies are generally underestimated in the valleys and overestimated on the hilltops. Second, the irregular sampling geometry was found to introduce some degree of aliasing (Featherstone and Kirby 2000). In order to numerically counter these effects, the DEM (Sect. 2.3), which gives a better representation of the mean terrain height than the gravity observation elevations, was used to reconstruct mean free-air gravity anomalies (Featherstone and Kirby 2000). The negative Bouguer correction for the mean height of each DEM cell was used to compute a 9 by 9 arc-second grid of mean free-air gravity anomalies from the 9 by 9 arc-second grid of interpolated simple Bouguer gravity anomalies.

The 9 by 9 arc-second grid of mean free-air gravity anomalies and the 27 by 27 arc-second grid of terrain corrections were then generalised and added onto a 2 by 2 arc-minute grid to yield mean Faye gravity anomalies. In the reconstruction technique and computation of mean Faye gravity anomalies (Featherstone and Kirby 2000), the terrain correction is not applied to the Bouguer gravity anomaly prior to gridding. This is because the terrain corrections applied to point gravity observations in a compartment are not necessarily representative of the integral mean value over the whole compartment. It is argued here that by including terrain information from areas not sampled by a gravity meter in the above ways, both the spatial resolution and accuracy of the computed grid of mean Faye gravity anomalies can be increased. However, a penalty of this approach is that the interpolation of simple Bouguer gravity anomalies is subject to some degree of aliasing. Accordingly, the stage at which the terrain correction is applied in this process remains an open question.

### 3.3 Combination of terrestrial and satellite altimeter-derived gravity data

Even though AUSGeoid98 is primarily for use on the Australian continent, accurate and dense marine gravity data are required to compute the best possible geoid solution on land in areas close to the coast. AUSGeoid91 and AUSGeoid93 relied on only a portion of the AGSO marine gravity data for geoid computation near the coast. The  $0.5^\circ$  spherical cap radius dictated this, as well as the computational strategy implemented in the ring integration software developed at the University of New South Wales. For AUSGeoid98, the AGSO marine gravity data coverage (Fig. 1b) was supplemented by satellite altimeter-derived marine gravity anomalies (Sect. 2.4), thus providing a much improved spatial coverage and resolution of marine gravity data.

Simple averaging of the AGSO marine gravity anomalies and the altimeter-derived gravity anomalies did not appear to improve the gravimetric geoid solution on land near the coast. This was concluded from comparisons of preliminary gravimetric geoid models, including and excluding the altimeter data, with GPS and AHD data around the coast of Australia. This result is most probably due to the relatively poor altimeter-derived gravity anomalies close to the coast. This degradation is caused by a combination of large and poorly modelled tides, backscatter from the land that prevents the accurate measurement of the radar returns, and altimeter loss of lock as the footprint passes over the coastal zone. The resulting errors in the altimeter-derived gravity anomalies are suspected to be of long and medium wavelength. Therefore, the computed geoid is degraded because the Stokes kernel, or a modification thereof applied over a limited area, does not completely attenuate the effects of any low-frequency errors in the terrestrial gravity field (cf. Vaníček and Featherstone 1998).

Instead of simple averaging, the AGSO gravity anomalies and altimeter-derived gravity anomalies were combined using a process termed 'draping' (see e.g. Kirby and Forsberg 1998). This procedure essentially involves gridding the differences between the two data sets using least squares collocation, then adding this difference back to the altimeter grid. The GRAVSOF software suite (see e.g. Tscherning et al. 1992) was used for this procedure with an empirically determined correlation length of 50 km and noise of 5 mGal.

An equally important consideration is the quality of the ship-track gravity data, where there were obvious linear drifts in the AGSO marine data due to the lack of sufficient cross-overs a long way offshore (cf. Wessel and Watts 1988). After a simple visual comparison of the AGSO and altimeter-derived gravity anomalies, approximately 25% of the AGSO data were discarded, all of which lay outside an approximate  $2^\circ$  zone around the Australian coastline (cf. Fig. 1b). It is accepted that this data-editing procedure is rather crude, but the AGSO marine gravity data records were not stored in a format to allow a cross-over analysis and adjustment to be performed.

Finally, it is acknowledged that another explanation for the observed deficiency may come from the conversion of sea surface heights, which are the direct measurements taken by the satellite altimeter, to gravity anomalies (see e.g. Sandwell and Smith 1997; Knudsen and Andersen 1998), and then the conversion of these to geoid heights. At present, it is unknown how errors, such as poorly modelled sea surface topography, propagate through the approximations used in these processes. However, from comparisons with GPS and AHD data around the coast of Australia, the use of the draped gravity anomalies gave preliminary geoid models that improved upon those obtained when using the averaged AGSO and altimeter-derived data or the AGSO data alone. Therefore, the draping approach offers a computationally convenient compromise to the improvement of coastal geoid solutions until improved altimeter tracking and solutions to the altimetry-gravimetry boundary-value problem are refined.

### 3.4 Summary

The computation of mean Faye gravity anomalies (as an approximation of mean Helmert gravity anomalies at the geoid) from point gravity observations is an involved process, especially for a continent the size of Australia. On land, point simple Bouguer gravity anomalies were computed and interpolated onto the same 9 by 9 arc-second grid as used for the DEM. The mean heights of the DEM elements were used to reconstruct a mean free-air gravity anomaly at each of the grid nodes. These and the 27 by 27 arc-second grids of terrain corrections and secondary indirect effects were then generalised onto a 2 by 2 arc-minute grid (approximately 3.7 km), which was used in the computation of AUSGeoid98 (Sect. 4). In marine areas, the AGSO gravity anomalies were combined with satellite altimeter-derived gravity anomalies using least squares collocation. Together, these approaches yielded a 2 by 2 arc-minute grid of mean gravity anomalies in the region bound by  $108^\circ\text{E}$  to  $160^\circ\text{E}$  and  $8^\circ\text{S}$  to  $45^\circ\text{S}$ .

Due to this elaborate series of processes, reliable estimates of the precision of this grid of mean gravity anomalies are difficult to determine, but are 'guestimated' to be accurate to approximately 2–3 mGal. The gravity anomalies implied by the degree-360 expansion of the EGM96 global geopotential model were subtracted from these terrestrial gravity anomalies prior to the geoid computations [Eq. (6)]. This included a  $-0.15$  mGal zero-degree term, which accounts for the difference in mass, but not the potential, between the EGM96 and GRS80 (Kirby and Featherstone 1997). Finally, it is important to point out that the computation of this grid of residual gravity anomalies proved to be the most time-consuming process in the production of AUSGeoid98. Therefore, this stage should always be factored into the total time taken to compute any gravimetric geoid model.

#### 4 Computation of the gravimetric geoid model

Over the last 15 years, two arguably ‘competing’ approaches to the use of a global geopotential model in regional gravimetric geoid computations have appeared in the geodetic literature.

- (1) The apparently most popular approach uses the complete expansion of a combined global geopotential model, which has been computed from a combination of satellite-derived and terrestrial gravity and terrain data (see e.g. Lemoine et al. 1998). These high-degree, typically degree-360, global geopotential models have generally been used in conjunction with the (unmodified) spherical Stokes kernel to compute the regional geoid, as was the case for AUSGeoid91 and AUSGeoid93. Due to the computational efficiencies achieved with the FFT, such regional geoid models now use gravity data over the whole area in which the geoid is required. Examples of FFT-based regional gravimetric geoid solutions that use a combined global geopotential model, a spherical Stokes kernel and the whole rectangular gravity data grid have been computed for the Nordic area (Forsberg 1990), Canada (Sideris and She 1995), the USA (Smith and Milbert 1999) and East Africa (Gachari and Olliver 1998).
- (2) The other approach to the use of a global geopotential model in regional geoid computation is to take only the low-degree expansion, typically to degree-20, of a satellite-only model in conjunction with integration of terrestrial gravity data over a limited spherical cap using a modified form of Stokes’s integral. A truncated expansion of a combined global geopotential model, typically to degree-120, is used to compute the contribution to the geoid from the remote zones. This truncated expansion only needs to be used because the spherical harmonic terms beyond degree-120 become negligible due to the kernel modification. An example of such a gravimetric geoid solution has been computed for Canada (Vaniček et al. 1995).

There are many convincing arguments in favour of and against either of these approaches, which will not be duplicated here. However, it is important to note that each approach appears to give similar fits to GPS and orthometric height data, where they have been tested in such a way. AUSGeoid98 is novel in that it was computed using a combination of the above two approaches, which aims to exploit the perceived benefits of each. This will be called the ‘hybrid approach’ (Sect. 4.4) and appears to deliver better results for Australia when the resulting gravimetric geoid is compared to GPS and spirit levelling data on the AHD (Sect. 5).

AUSGeoid98 uses the degree-20 component of the EGM96 global geopotential model to define the reference spheroid as per the generalised Stokes scheme (Sect. 4.1). This truncation is chosen somewhat arbitrarily, but is based on the value used by Vaniček et al. (1995) who describe the justification for its use. The remaining expansion of EGM96 to degree-360 was used in a remove–

compute–restore stage residual to this reference spheroid (Sect. 4.4).

Forsberg and Featherstone (1998) and Forsberg (1998) show that the use of a spherical cap of radius  $\psi_0$  about each computation point is preferable for Australian geoid computations (Sect. 4.2). This is instead of using the whole rectangular gravity data grid, which delivers better results than a spherical cap in other parts of the world such as Scandinavia (Forsberg and Featherstone 1998). Associated with the use of a limited spherical cap, a modified Stokes’s kernel (Sect. 4.3) was used to further reduce the truncation error, in addition to the use of the degree-360 expansion of the EGM96 global geopotential model. The spherical cap also adapts the filtering properties of the kernel to reduce the propagation of terrestrial gravity data errors into the geoid solution (Vaniček and Featherstone 1998). This is supported by the results presented in Sect. 5 when using Australian data.

##### 4.1 The generalised Stokes scheme

Stokes’s solution to the geodetic boundary-value problem was formulated for terrestrial gravity anomalies in a spherical approximation. Therefore, even if a spatially dense global coverage of terrestrial gravity anomalies were readily available, a global integration would introduce an error in the computed geoid heights of the order of the flattening of the reference ellipsoid ( $\sim 0.34\%$ ). However, the availability of (low-frequency) global gravity field information from the analysis of the orbits of artificial Earth satellites has provided a more attractive and practical alternative.

In this case, the Stokes integral is evaluated residual to a global geopotential model using terrestrial gravity data over the region of interest (see e.g. Vincent and Marsh 1973). However, the use of the spherical Stokes kernel in conjunction with a global geopotential model allows the unattenuated propagation of low-frequency errors in the terrestrial gravity data into the geoid solution (Vaniček and Featherstone 1998). Given that the satellite-derived gravity data are widely acknowledged to be the better source of low-frequency gravity field information, it becomes preferable to reformulate the geodetic boundary-value problem for a higher than second-degree reference spheroid (Martinec and Vaniček 1997).

The solution to this boundary-value problem forms the generalised Stokes scheme (Vaniček and Sjöberg 1991) which is expressed for a global integration as

$$N = N_M + \frac{R}{4\pi\gamma} \int_{\sigma} S^{M+1}(\psi) \Delta g^{M+1} d\sigma \quad (4)$$

where  $N_M$  is the contribution of the reference spheroid to the geoid height with respect to the reference ellipsoid, which is provided by a low-degree and low-order ( $M = 20$  in the case of AUSGeoid98) expansion of a global geopotential model according to

$$N_M = \frac{GM}{r^\gamma} \sum_{n=2}^M \left(\frac{a}{r}\right)^n \times \sum_{m=0}^n (\delta\bar{C}_{nm} \cos m\lambda + \bar{S}_{nm} \sin m\lambda) \bar{P}_{nm}(\cos \theta) \quad (5)$$

The residual gravity anomalies ( $\Delta g^{M+1}$ ) are computed from the terrestrial gravity anomalies ( $\Delta g$ ) according to

$$\Delta g^{M+1} = \Delta g - \frac{GM}{r^2} \sum_{n=2}^M \left(\frac{a}{r}\right)^n (n-1) \times \sum_{m=0}^n (\delta\bar{C}_{nm} \cos m\lambda + \bar{S}_{nm} \sin m\lambda) \bar{P}_{nm}(\cos \theta) \quad (6)$$

which must use the same degree of expansion of the same geopotential coefficients used for the reference spheroid [Eq. (5)]. In Eqs. (5) and (6),  $GM$  is the geocentric gravitational constant,  $(r, \theta, \lambda)$  are the geocentric spherical polar coordinates of the computation point,  $\bar{P}_{nm}$  are the fully normalised associated Legendre polynomials for degree  $n$  and order  $m$ , and  $\delta\bar{C}_{nm}$  and  $\bar{S}_{nm}$  are the fully normalised spherical harmonic coefficients of the geopotential model that have been reduced by the even zonal harmonics of the reference ellipsoid.

From a practical point of view, the spheroidal Stokes kernel  $S^{M+1}(\psi)$  in Eq. (4), which is implicit to the generalised Stokes scheme, can be computed simply by removing the low-degree Legendre polynomials [ $P_n(\cos \psi)$ ] from the closed form of the spherical Stokes kernel

$$S^{M+1}(\psi) = S(\psi) - \sum_{n=2}^M \frac{2n+1}{n-1} P_n(\cos \psi) \quad (7)$$

where  $S(\psi)$  is the spherical Stokes kernel (Heiskanen and Moritz 1967, p. 94) and  $\psi$  is the spherical distance between the computation point and the remote points in Eq. (4).

The spheroidal Stokes kernel [Eq. (7)] acts as a high-pass filter that completely eliminates low-frequency errors in the terrestrial gravity data only when a global integration is performed (Vaniček and Featherstone 1998). It is important to note that this condition breaks down when the integration is performed over a limited area, where only a proportion of the low-degree terrestrial gravity data errors are high-pass filtered from the geoid model. Nevertheless, the generalised Stokes scheme is considered a more desirable approach to gravimetric geoid determination in Australia because of the errors in the Australian gravity data (Sects. 2.2 and 3.2; also see Sect. 5). The generalised Stokes scheme is also suited to evaluation by the 1-D-FFT technique after using only minor adaptations to existing techniques for the spherical Stokes kernel (Sect. 4.3).

As stated, the generalised Stokes approach also reduces the impact of the spherical approximation error (Vaniček and Sjöberg 1991). This is because the spherical approximation error of  $\sim 0.34\%$  now only applies to

the computed residual geoid heights (at most 5 m in Australia) instead of the total geoid height (at most 80 m in Australia) since most of the geoid's power is contained within the low frequencies. Recently, there has been some renewed interest in the computation of ellipsoidal corrections to the spherical Stokes integral to account for this spherical approximation error. However, the formulae that are currently receiving attention (see e.g. Fei and Sideris 2000) were not available at the time that AUSGeoid98 was computed. Instead, the use of the generalised Stokes scheme is assumed to reduce the spherical approximation error to an acceptable level in relation to the expected accuracy of the AHD (Sect. 2.5). Nevertheless, further work is required to formulate and compute, rather than neglect, ellipsoidal corrections to the generalised Stokes formula.

#### 4.2 Limited spherical integration caps in the 1-D-FFT technique

Undoubtedly, the FFT technique has provided an efficient means with which to compute regional gravimetric geoid models over large areas (see e.g. Schwarz et al. 1990). Previously, the 2-D-FFT was used through a planar approximation of the spherical Stokes kernel, which introduces errors for geoid computations over a region of the size of Australia (see e.g. Tziavos 1996). However, the 1-D-FFT technique (Haagmans et al. 1993) avoids this approximation error. Therefore, the 1-D-FFT technique has been used for the computation of AUSGeoid98. It is acknowledged that more efficient quadrature-based numerical integration techniques are now available (Huang et al. 2000), but these were not available at the time that AUSGeoid98 was computed.

Comparisons of 1-D-FFT computer software with quadrature-based numerical integration software show near-identical results, while providing a significant increase in computational efficiency. For instance, to compute a gravimetric geoid on a 2 by 2 arc-minute grid over Australia (108°E to 160°E and 8°S to 45°S) using the 1-D-FFT takes approximately three days on a Sun Ultra 1 work-station (128 Mb RAM, 148 MHz CPU). Conversely, it would take (an estimated) few weeks to compute the same grid using quadrature-based numerical integration on the same computer, only to achieve the same results.

AUSGeoid91 and AUSGeoid93 used quadrature-based numerical integration, but restricted computer power and availability at the time drove the computation of 10 by 10 arc-minute grids of geoid undulations. However, interpolation of geoid heights from these coarse grids was found to cause errors in the transformation of GPS-derived heights to the AHD (Freund et al. 1997). Therefore, AUSGeoid98 has been computed on a 2 by 2 arc-minute grid. This has been allowed by the efficiency gains delivered by the 1-D-FFT, as well as the improvements in computer performance at reduced capital costs. As the 'users' demand more accurate interpolation of geoid heights from pre-computed grids, and more accurate gravity field information becomes

available, future Australian geoid models may need to be computed at an even higher spatial resolution.

As stated, gravimetric geoid models computed in other parts of the world using FFT techniques and the spherical Stokes kernel often use the whole regional gravity data set (see e.g. Forsberg 1990; Sideris and She 1995; Gachari and Olliver 1998; Smith and Milbert 1999). While this approach appears to be appropriate in these regions (as determined from comparisons with GPS and spirit-levelling data on the local vertical datums), a considerably worse result is achieved in Australia when using the whole Australian gravity data rectangle (Forsberg 1998, Forsberg and Featherstone 1998).

This is a slightly unexpected result because it is reasonable to assume that the more data that are used (i.e. the larger the integration domain), the better the geoid solution, especially towards the centre of the computation area where the truncation error becomes smaller. This result is most probably due to a combination of the unattenuated propagation of systematic errors in the Australian gravity data (Sects. 2.2 and 3.2) by the spherical Stokes kernel (Vaniček and Featherstone 1998), as well as distortions in the AHD (see e.g. Featherstone 1998; Featherstone and Stewart 1998, Sect. 5.3 of the present paper).

Accordingly, it was found necessary to implement a spherical cap of limited spatial extent ( $\psi_0$ ) in the 1-D-FFT for geoid computations in Australia. This was achieved simply by setting the value of the Stokesian kernel to zero outside the cap before it is transformed to the frequency domain (cf. Featherstone and Sideris 1998). This makes the 1-D-FFT technique more closely resemble quadrature-based numerical integration over a limited spherical cap. It also limits the propagation of FFT edge effects into the geoid solution (cf. Sideris and Li 1993). Instead, these edge effects are restricted to a band equal to the cap radius from the edge of the gravity data rectangle.

The penalty of using a smaller integration domain for all geoid computation points is that the truncation error is increased for those points towards the centre of the gravity data rectangle, whereas it would normally be reduced when using the whole gravity data rectangle. However, based on the results of using limited spherical caps in the 1-D-FFT technique over Australia (Sect. 5), the truncation error appears to be smaller than the terrestrial gravity data errors propagated when using a larger integration domain. Clearly, this presents an optimisation problem, which will be addressed empirically in terms of the integration radius in Sect. 5.1.

### 4.3 The deterministically modified Stokes kernel in the 1-D-FFT

As mentioned, gravimetric geoid determination demands that detailed gravity data are used from over the whole Earth, which applies to both the spherical Stokes and the generalised [Eq. (4)] Stokes integrals. However, due to reasons of restricted field access and data confidentiality, this is not currently possible and is unlikely to be achieved in the near future. Therefore, a

limited data area is inevitably used in regional geoid computations with this approximation resulting in the truncation error, irrespective of the computational approach or theory used. The truncation error can be reduced through the use of a high-degree global geopotential model, a modification to Stokes's kernel, or a combination of these; the last of these was used for AUSGeoid98 (Sect. 4.4).

Historically, kernel modifications were designed to reduce the truncation error, but they also adapt the kernel to yield some preferable high-pass filtering properties (Vanicek and Featherstone 1988). Two distinct classes of kernel modification have been introduced since the pioneering work of Molodensky, which take deterministic and stochastic approaches (many of which are cited in Featherstone et al. 1998). The stochastic modifications (see e.g. Sjöberg and Hunegnaw 2000 and the references cited therein) were not used because reliable estimates of the error variances of the Australian gravity data are not currently known.

The deterministic kernel modification of Featherstone et al. (1998) was used in the computation of AUSGeoid98 because it offers a combination of the benefits of several existing deterministic modifications. To summarise, it makes a least squares minimisation of the upper bound of the truncation error (Vaniček and Kleusberg 1987; Vaniček and Sjöberg 1991), while also causing the Fourier series of this truncation error to converge to zero more rapidly (cf. Evans and Featherstone 2000). Therefore, when also using a high-degree global geopotential model, the truncation error is assumed reduced to the point that it can be ignored (Sect. 4.4).

The Featherstone et al. (1998) modified kernel requires that the kernel is zero at the truncation radius ( $\psi_0$ ), and is given by

$$S_F^{M+1}(\psi, \psi_0) = S_V^{M+1}(\psi) - S_V^{M+1}(\psi_0) \quad \text{for } 0 \leq \psi \leq \psi_0 \quad (8)$$

where

$$S_V^{M+1}(\psi) = S^{M+1}(\psi) - \sum_{k=2}^M \frac{2k+1}{2} t_k(\psi_0) P_k(\cos \psi) \quad (9)$$

is the Vaniček and Kleusberg (1987) modified kernel and  $S^{M+1}(\psi)$  is given by Eq. (7). The  $t_k(\psi_0)$  modification coefficients in Eq. (9) were first derived by Vaniček and Kleusberg (1987) and can be evaluated from the solution of the following set of  $M$  linear equations:

$$\begin{aligned} & \sum_{k=2}^M \frac{2k+1}{2} t_k(\psi_0) e_{nk}(\psi_0) \\ & = Q_n(\psi_0) - \sum_{k=2}^M \frac{2k+1}{k-1} e_{nk}(\psi_0) \end{aligned} \quad (10)$$

where both

$$e_{nk}(\psi_0) = \int_{\psi_0}^{\pi} P_k(\cos \psi) P_n(\cos \psi) \sin \psi \, d\psi \quad (11)$$

and

$$Q_n(\psi_0) = \int_{\psi_0}^{\pi} S(\psi) P_n(\cos \psi) \sin \psi \, d\psi \quad (12)$$

can be computed using Paul's (1973) algorithms.

The use of Eq. (8) in Eq. (4) over a limited spherical cap  $\sigma_0$  of radius  $\psi_0$  about each geoid computation point leads to the following approximation of the geoid height:

$$N \approx N_M + \frac{R}{4\pi\gamma} \int_{\sigma_0} S_f^{M+1}(\psi, \psi_0) \Delta g^{M+1} \, d\sigma \quad (13)$$

the truncation error term due to the modified spheroidal Stokes integral in the region  $(\sigma - \sigma_0)$ , which is omitted from Eq. (13), will be discussed in relation to the hybrid approach (Sect. 4.4).

For AUSGeoid98, the degree of deterministic kernel modification in Eq. (9) was chosen to be  $M = 20$ , which is the same as the degree of spheroid used in the generalised Stokes scheme [Eq. (4)], thus avoiding the need to compute additional terms (cf. Evans and Featherstone 2000). It is acknowledged that the modified kernel reduces the effectiveness of the high-pass filtering properties of the spheroidal Stokes kernel (Vaniček and Featherstone 1998), which is a penalty of reducing the truncation error. Nevertheless, the modified kernel is still a more effective (partial) high-pass filter of terrestrial gravity data errors than the spherical Stokes kernel, which is not a high-pass filter. Figure 2 shows a plot of the spherical Stokes kernel (Heiskanen and Moritz 1967, p. 94), the  $M = 20$  spheroidal Stokes kernel [Eq. (7)] and the  $M = 20$  Featherstone et al. (1998) kernel [Eq. (8)] for a spherical cap radius of  $\psi_0 = 1^\circ$ .

Equation (8) was implemented in the University of Calgary's 1-D-FFT geoid computation software (Sideris 1994) by evaluating it in the space domain before Fourier transformation to the frequency domain (cf. Featherstone and Sideris 1998). In order to implement the spherical cap (Sect. 4.2), the values of the modified Stokes kernel were set to zero beyond  $\psi_0$  before transformation to the frequency domain. [It is acknowledged here that the results presented in Featherstone and Sideris (1998) are subject to some gross errors in the GPS and AHD data used. However, the conclusions reached are still correct, which was verified by a re-evaluation of the techniques compared with corrected GPS-AHD data.]

An additional benefit of using the Featherstone et al. (1998) kernel or any other Meissl-like kernel modification in the FFT technique is that the kernel smoothly tends to zero at the cap radius. This reduces the Gibbs phenomenon that results when the spherical Stokes or other kernel is truncated at a non-zero value before Fourier transformation. This is because the Meissl-type modifications deliberately make the kernel a continuous function, whereas the truncated spherical Stokes kernel introduces a discontinuous function (cf. Evans and Featherstone 2000). The empirically determined im-

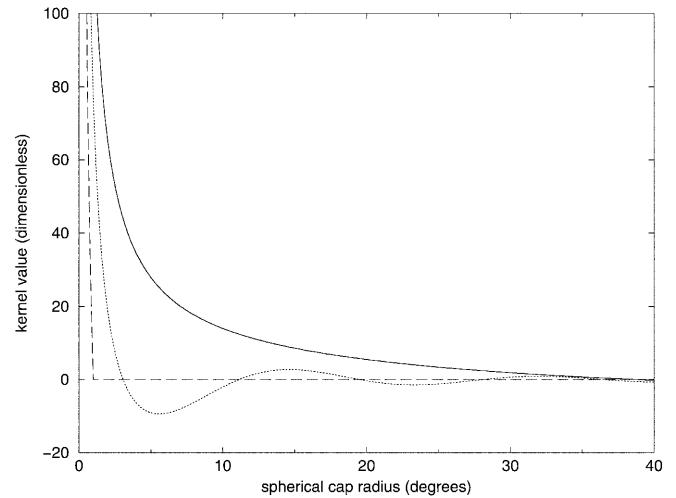


**Fig. 2.** The spherical Stokes kernel (*solid line*), the  $M = 20$  spheroidal Stokes kernel (*dotted line*) and the  $M = 20$  Featherstone et al. (1998) kernel for  $\psi_0 = 1^\circ$  (*dashed line*)

provements offered by the Featherstone et al. (1998) modified kernel over the spherical Stokes kernel will be presented in Sect. 5.1.

#### 4.4 The hybrid approach: remove–compute–restore in the generalised Stokes scheme with a modified kernel

Previous practical implementations of the generalised Stokes scheme (e.g. Vanicek et al. 1995) use an  $M = 20$  reference spheroid, integration over a limited spherical cap using a modified integration kernel, and a direct evaluation of the corresponding truncation error term. For AUSGeoid98 it was decided instead to use a variant of the so-called remove–compute–restore technique based on an  $M = 20$  reference spheroid, together with the Featherstone et al. (1998) modified kernel and the complete expansion of a high-degree combined global geopotential model. This is simple to implement in practice, where the degree-360 expansion of the global geopotential model is first removed from the terrestrial gravity anomalies [Eq. (6)], then the residual geoid undulations are computed from these residual gravity anomalies using the  $M = 20$  deterministically modified kernel [Eq. (8)] in the 1-D-FFT.

For AUSGeoid98, the degree-20 component of the EGM96 geoid provides the reference spheroid implicit to the generalised Stokes scheme, while the degree-21 to degree-360 components of the EGM96 geoid and gravity anomalies are used in the remove–compute–restore scheme. This approach, coupled with the increased rate of convergence of the truncation error due to the kernel modification, then allows the truncation error term for spherical harmonic degrees greater than 360 to be ignored completely. Therefore, Eq. (13) becomes

$$N = N_{M_{\max}} + \frac{R}{4\pi\gamma} \int_{\sigma_0} S_f^{M+1}(\psi, \psi_0) \Delta g^{M_{\max}+1} \, d\sigma \quad (14)$$

where  $M_{\max}$  indicates that the maximum spherical harmonic expansion of the coefficients available in the global geopotential model is used in Eqs. (5) and (6). The degree of kernel modification [Eq. (8)] remains at  $M = 20$ . The 1-D-FFT implementation of Eq. (14) is adapted from Haagmans et al. (1993) to give

$$N = N_{M_{\max}} + \frac{R\Delta\phi\Delta\lambda}{4\pi\gamma} \mathbf{F}^{-1} \times \left[ \sum \mathbf{F}\{S_F^{M+1}(\psi, \psi_0)\} \mathbf{F}\{\Delta g^{M_{\max}+1} \cos \phi\} \right] \quad (15)$$

where  $\Delta\phi$  and  $\Delta\lambda$  are the grid spacings in latitude and longitude (both 2 arc-minutes for AUSGeoid98),  $\mathbf{F}$  and  $\mathbf{F}^{-1}$  are the forward and inverse 1-D-FFT operators, respectively, which are performed in the longitudinal direction, and  $\sum$  denotes the summation performed in the latitudinal direction. By way of comparison, the 1-D-FFT implementation of the ‘conventional’ remove–compute–restore technique with a spherical Stokes kernel is

$$N = N_{M_{\max}} + \frac{R\Delta\phi\Delta\lambda}{4\pi\gamma} \mathbf{F}^{-1} \times \left[ \sum \mathbf{F}\{S(\psi)\} \mathbf{F}\{\Delta g^{M_{\max}+1} \cos \phi\} \right] \quad (16)$$

which will be used for the empirical tests presented in Sect. 5.1.

Featherstone (1999) demonstrates that this ‘hybrid approach’ [Eq. (15)] is preferable to the ‘conventional’ remove–compute–restore technique based on the spherical Stokes kernel [Eq. (16)]. This uses a set of self-consistent geoid heights and gravity anomalies that have been derived from a synthetic gravity field model based on spherical harmonics. Importantly, the hybrid approach shows a slight improvement over the approach of using a degree-360 global geopotential model with the spherical Stokes kernel and the whole grid of gravity anomalies. Section 5.1 shows the results of a similar empirical investigation of the hybrid approach and spherical caps using Australian data.

#### 4.5 Summary

A hybrid approach to the generalised Stokes scheme [Eq. (4)] with a deterministically modified Stokes kernel [Eq. (8)] and the remove–compute–restore technique based on a higher-degree global geopotential model [Eq. (14)] was used in the computation of AUSGeoid98. This was implemented numerically using the 1-D-FFT technique [Eq. (15)]. The degree  $M = 20$  expansion of EGM96 was used to provide the reference spheroid in the generalised Stokes scheme. The  $M_{\max} = 360$  expansion of the EGM96 global geopotential model was used in the remove–compute–restore technique based on the  $M = 20$  reference spheroid.

The Featherstone et al. (1998) deterministically modified kernel [Eq. (8)], also based on an  $M = 20$  reference spheroid, was used over a spherical cap of limited

radius  $\psi_0$ . This approach was adopted to reduce the truncation error so that it can be ignored, while also adapting the filtering properties of the kernel to reduce the propagation of low-frequency errors from the terrestrial gravity data. Comparisons of AUSGeoid98 with GPS and AHD data (shown next) were used to empirically optimise  $\psi_0$ , and also to indicate that this hybrid approach was appropriate for Australian data.

## 5 Comparisons of AUSGeoid98 with GPS–AHD heights

As is customary with gravimetric geoid validations on land, co-located GPS ellipsoidal heights and spirit-levelled heights on the AHD were used as control on the computation of AUSGeoid98. The geoid–GRS80-ellipsoid separations, given by the AUSGeoid93 and AUSGeoid98 gravimetric geoid models, are compared with the discrete AHD–GRS80-ellipsoid separations, which were determined geometrically from the GPS and AHD data. However, recall that such an approach should not be relied upon unequivocally, since the GPS and AHD data have their own error budgets.

This approach to geoid validation on land is also questionable because a local vertical datum is not necessarily coincident with the geoid as classically defined, which is the case in Australia (e.g. Featherstone 1998). Nevertheless, these data currently offer the only means of verifying gravimetric geoid solutions on land. Moreover, such a validation gives an indication of the performance of AUSGeoid98 in its primary application of transforming GPS-derived ellipsoidal heights to the AHD and vice versa.

It is worth noting that the subsequent tests use nationwide sets of GPS–AHD control data comprising 906 points (Johnston and Featherstone 1998a, b) and 1013 points (Featherstone and Guo submitted). However, the techniques and theories developed to achieve the improved fit to GPS and AHD data used a nationwide subset of 141 GPS–AHD heights as control. These were the only reliable data available to the authors at the time. The use of the additional GPS–AHD data has allowed AUSLIG to perform its own verifications of AUSGeoid98 before it was released to the Australian public. It is argued that this is a preferable scenario because it enables some, partially independent, verification of the geoid computations. Since the production of AUSGeoid98, an additional 107 GPS–AHD heights have been acquired. Therefore, the subsequent sections will present the results using the data sets comprising 906 and 1013 GPS–AHD heights. The spatial coverage of these GPS–AHD data sets is shown in Fig. 3.

### 5.1 Empirical optimisation of the integration cap radius

With any geoid determination theory, it is useful to empirically verify the expected improvements using observational data. In the practical application of the ‘hybrid approach’ (Sect. 4.4), the parameters that could

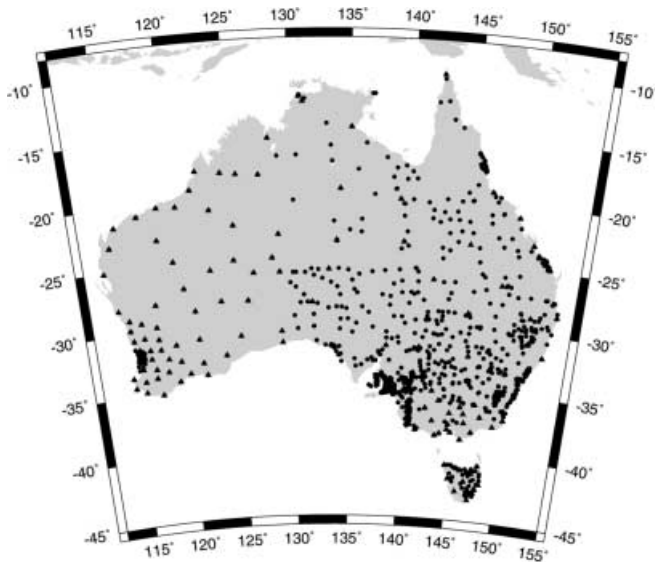


**Fig. 3.** Coverage of the GPS–AHD control data (Lambert conical projection). The 141 points (*triangles*) were used for preliminary testing in the AUSGeoid98 research phase. The 906 points (*circles*) were used for testing in the AUSGeoid98 production phase

be optimised include the degree of the reference spheroid ( $M$ ), the kernel modification [some of the many options are cited in Featherstone et al. (1998) and Sjöberg and Hunegnaw (2000)], and the radius of the spherical integration cap ( $\psi_0$ ). The degree of the reference spheroid was chosen to be  $M = 20$  (cf. Vaniček et al. 1995), as was the degree of the Featherstone et al. (1998) deterministic kernel modification [Eq. (8)]. This modification was selected because it is considered to advance on previous deterministic modifications since it combines several of them into a single scheme. Given the expected errors in the Australian gravity data (Sects. 2.2 and 3.2), a balance has to be achieved between the propagation of these errors versus the truncation error. Therefore, the integration cap radius ( $\psi_0$ ) remained the only parameter that was optimised in the computation of AUSGeoid98 (cf. Kearsley 1988a).

The lowest standard deviation of fit of the gravimetric geoid model to the GPS and AHD data is taken to indicate the optimal cap radius for the computation of AUSGeoid98, bearing in mind that it will be used on land mostly to transform GPS-derived heights to the AHD (Sect. 1). The standard deviation is used because these comparisons were conducted in an absolute sense (Sect. 2.5) and the mean difference can be attributed, in part, to the poor knowledge of the zero-degree term in the geoid (Sect. 5.2).

First, it is informative to investigate the use of the 1-D-FFT geoid computation technique with a limited spherical cap radius ( $\psi_0$ ) and a spherical Stokes kernel, as opposed to the use of the entire Australian gravity grid and a spherical Stokes kernel. This replicates, in part, the experiments conducted by Forsberg (1998) and Forsberg and Featherstone (1998). The gravimetric geoid models, computed either way, were compared with the nationwide set of 906 discrete AHD–GRS80-ellip-

soid separations in Fig. 3 (cf. Johnston and Featherstone 1998a, b).

Using the whole Australian gravity data rectangle (108°E to 160°E and 8°S to 45°S), in conjunction with the  $M_{\max} = 360$  expansion of the EGM96 global geopotential model and the spherical Stokes kernel [Eq. (16)], yields a standard deviation of fit to the 906 GPS and AHD data of  $\pm 1.113$  m. Using  $\psi_0 = 1^\circ$  and the spherical Stokes kernel in Eq. (16) yields a standard deviation of fit to the same GPS and AHD data of  $\pm 0.402$  m. Importantly, the standard deviation of fit to the GPS and AHD data achieved when using the whole gravity data grid is considerably worse than that achieved for the  $M_{\max} = 360$  expansion of EGM96 alone ( $\pm 0.458$  m), whereas the use of  $\psi_0 = 1^\circ$  makes a small improvement upon EGM96.

These results corroborate the findings of Forsberg (1998) and Forsberg and Featherstone (1998), and *vice versa*, who use different geoid computation software (Forsberg and Sideris 1993), different gravity data gridding (i.e. the terrain corrections were applied to the simple Bouguer anomalies before interpolation onto a grid), and some different GPS and AHD data. It is argued here that this observation is due to either long-wavelength errors in the Australian gravity data grid that are propagated directly into the geoid solution or distortions in the AHD, or to both. Given that the suspected distortions in the AHD are of the order of 1 m (see e.g. Featherstone 1998), these cannot account solely for the  $\pm 1.113$  m standard deviation observed when using the whole gravity data rectangle. Therefore, the poorer fit is more likely to be due to the Australian gravity data and gridding errors, coupled with the theoretically inappropriate use of the spherical Stokes kernel that allows these errors to propagate into the geoid solution (Vaniček and Featherstone 1998).

Next, the performance of the limited spherical cap is investigated when the geoid is computed using the hybrid approach [Eq. (15)]. This is compared with the spherical Stokes kernel and a limited cap in the conventional remove–compute–restore technique [Eq. (16)]. Figure 4 shows the standard deviation of the fit of geoid solutions to the 906 GPS–AHD data, computed using the modified [Eq. (8)] and spherical Stokes kernels, versus integration cap radius ( $\psi_0$ ). Recall that the smallest standard deviation of the fit of the gravimetric geoid model to the GPS–AHD data is used to select the optimal integration cap radius.

From Fig. 4, the improvement achieved when using the Featherstone et al. (1998) modification to the generalised Stokes scheme [Eq. (15)] over the ‘conventional’ remove–compute–restore technique [Eq. (16)] is evident from the standard deviation of the fit of the various gravimetric geoid models to the 906 GPS–AHD data across Australia. For  $\psi_0 = 1^\circ$  the use of the modified kernel yields the smallest standard deviation of fit of  $\pm 0.364$  m, whereas the use of the spherical Stokes kernel yields a standard deviation of fit of  $\pm 0.402$  m. By way of comparison, AUSGeoid93, which used  $\psi_0 = 0.5^\circ$ , gives a standard deviation of fit of  $\pm 0.510$  m, thus illustrating the improvements made by using more

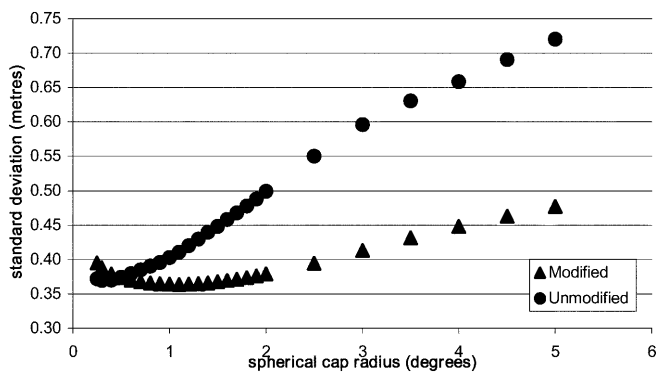


Fig. 4. Standard deviation of the fit of gravimetric geoid solutions, computed using the spherical and  $M = 20$  Featherstone et al. (1998) modified Stokes kernels with increasing  $\psi_0$ , to a nationwide set of 906 discrete GPS–AHD heights

recent data (Sect. 2), as well as the improvement due to the hybrid approach (Sect. 4.4).

With the exception of  $\psi_0 < 0.5^\circ$ , the modified integration kernel yields consistently better fits than the spherical Stokes kernel with increasing  $\psi_0$  (Fig. 4). The relatively poor performance of the modified kernel for small  $\psi_0$  is because of numerical instabilities in the computation of the modification coefficients [Eqs. (9)–(12)] at these radii. Importantly, however, the geoid solution using the modified kernel and  $\psi_0 = 1^\circ$  gives a better fit to the GPS–AHD data than the unmodified kernel for all radii tested (Fig. 4).

It is interesting to observe from Fig. 4 that the geoid solutions give progressively worse fits with increasing cap radius, irrespective of the approach used. This is attributed to a combination of errors in the AHD and the leakage of errors from the terrestrial gravity data into the geoid models. The latter occurs because the spherical cap also acts as a (partial) high-pass filter (cf. Vaniček and Featherstone 1998), with the amount of high-pass filtering increasing with decreasing cap radius. Therefore, larger cap radii in each geoid determination technique allow more errors to propagate from the terrestrial gravity data into the geoid solution. Despite this, the modified kernel is a more effective high-pass filter than the spherical Stokes kernel over a limited cap. Future work will seek to optimise the filtering properties of the kernel so as to reduce this effect on Australian geoid determination.

### 5.2 Geometrical estimation of the zero-degree term

Any gravimetric geoid is deficient in the zero-degree term, because the true mass of the Earth and potential of the geoid remains poorly known. Therefore, it is necessary to apply a constant bias to any gravimetric geoid in order to account for this. Zero-degree terms, which account only for the differing mass (and not the potential) of the GRS80 ellipsoid and the EGM96 global geopotential model (Kirby and Featherstone 1997), were used for both the geoid heights (0.937 m) and gravity anomalies ( $-0.15$  mGal) in the generalised Stokes

scheme (Sect. 4.1). Heiskanen and Moritz (1967) recommend using geometrical geoid information to control this term, which is available from the 906 Australian GPS–AHD data since the GPS networks have been geodetically tied to the ITRF92 (epoch 94.0).

This control on the zero-degree term was applied by calculating the mean difference between the gravimetric geoid computed using the hybrid approach [Eq. (15)] with  $M = 20$  and  $\psi_0 = 1^\circ$  and GPS–AHD control data in an absolute sense (Sect. 2.5). This gave 0.940 m, which is virtually identical to the (mass-only) zero-degree term calculated for EGM96 and GRS80 (Kirby and Featherstone 1997). By taking this approach, the gravimetric geoid solution is made more accurate in an absolute sense, but at the same time it is subjected to vertical datum deficiencies (cf. Rapp 1994) and any very-long-wavelength errors that manifest as a constant bias over Australia. However, this approach is important from a practical point of view so that the users of AUSGeoid98 who conduct GPS surveys with respect to existing control do not have to deal with a  $\sim 1$ -m offset.

### 5.3 Regional comparisons with GPS–AHD data

Given that the primary application of AUSGeoid98 is to transform GPS-derived ellipsoidal height differences to AHD height differences and *vice versa*, relative comparisons (Sect. 2.5) were made over baselines less than 200 km in length. This analysis is restricted to using subsets of the 906 GPS–AHD data in areas where the transfer of vertical geodetic control using GPS was previously known to be poor with AUSGeoid93. These areas are the Adelaide hills ( $\sim 138^\circ\text{E}$ ,  $\sim 33^\circ\text{S}$ ), southern Australian Capital Territory ( $\sim 147^\circ\text{E}$ ,  $\sim 35^\circ\text{S}$ ), the Brisbane area ( $\sim 153^\circ\text{E}$ ,  $\sim 27^\circ\text{S}$ ), the Cairns area ( $\sim 146^\circ\text{E}$ ,  $\sim 18^\circ\text{S}$ ), the Perth area ( $\sim 116^\circ\text{E}$ ,  $\sim 32^\circ\text{S}$ ), and the southern New South Wales region ( $\sim 147^\circ\text{E}$ ,  $\sim 34^\circ\text{S}$ ). Figure 5 shows the differences between GPS–AHD height differences and gravimetric geoid height differences for AUSGeoid93 and AUSGeoid98 in relation to the third-order spirit-levelling tolerance used in Australia (Sect. 1).

From Fig. 5 it can be seen that AUSGeoid98 generally gives an improvement over AUSGeoid93, although this is not always the case. This partly reflects the effect of errors in the AHD control data on relative comparisons of geoid models. Given that the AHD is a third-order vertical datum, most of the differences in Fig. 5 can be accommodated solely within the Australian third-order spirit-levelling tolerance. In Fig. 5, the differences between AUSGeoid93 and AUSGeoid98 are less than the third-order levelling tolerance (solid line). As such, it is slightly more informative to use average values.

The average allowable misclose under the third-order spirit-levelling specification for the baselines used in Fig. 5 is 48.6 mm. The average difference between AUSGeoid98 and the GPS–AHD data over the same baselines is 57.2 mm, whereas AUSGeoid93 yields an average difference of 155.7 mm. Therefore, AUSGeoid98 provides an *overall* improvement on AUSGeoid93 for the trans-

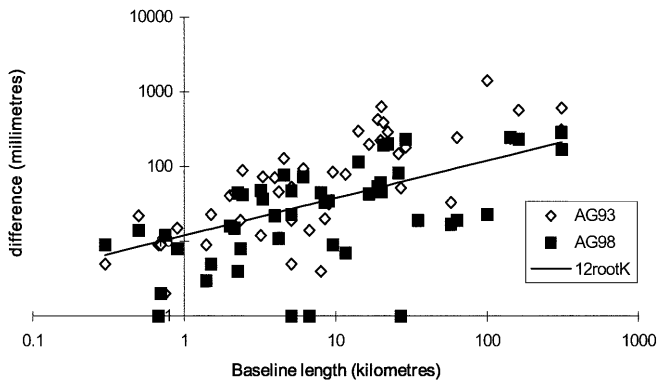


**Fig. 5.** Differences between GPS–AHD height differences and AUSGeoid93 and AUSGeoid98 geoid height differences for baseline lengths less than 200 km in selected regions of Australia (logarithmic scale)

formation of GPS-derived height differences to AHD height differences in these previously problematic regions of Australia.

Further examination of AUSGeoid98 in the Perth metropolitan region revealed that, although AUSGeoid98 made an improvement on AUSGeoid93, it did not satisfy the requirements of the Western Australian Department of Land Administration. This is due to the presence of the Darling Fault, which causes an extremely steep geoid–GRS80-ellipsoid gradient of approximately 100 mm/km. Therefore, following the arguments in Featherstone (1998), a model of the separation of the AHD and GRS80 ellipsoid was constructed using 99 additional GPS–AHD heights that were not used in the above analyses.

This combination used least squares collocation to model the differences between the gravimetric version of AUSGeoid98 and the AHD in this region (Featherstone

2000). This is analogous with the ‘draping’ used to merge the AGSO and satellite altimeter data (Sect. 3.3), and used the GRAVSOFT package (Tscherning et al. 1992) with a correlation length of 15 km and  $\pm 11$  mm noise. This approach improved the standard deviation of the fit to the 99 GPS–AHD data from  $\pm 128$  to  $\pm 8$  mm. However, it must be borne in mind that this level of improvement is over-optimistic because the same GPS–AHD data have been used to both produce and verify the combined model. This combined model in the Perth region has been interfaced seamlessly with the version of AUSGeoid98 that was released to the public by AUSLIG in November 1998.

#### 5.4 Investigation of systematic differences between AUSGeoid98 and the AHD

Featherstone and Guo (submitted) perform some more detailed comparisons of AUSGeoid93 and AUSGeoid98 using a set of 1013 GPS–AHD data, which includes the 99 GPS–AHD data used to compute the combined model in the Perth region. The results from this study that are pertinent to the possible identification of systematic differences between AUSGeoid98 and the AHD are summarised here, and it is assumed that the errors in the GPS heights can be neglected.

First, Fig. 6 shows the absolute differences between the 1013 GPS–AHD data and AUSGeoid98. This reveals some systematic differences that are defined by more than one GPS–AHD point. Given that the known deficiencies in the AHD can reach  $\sim 1$  m (see e.g. Featherstone 1998), these could account for most of the differences shown in Fig. 6. However, it is possible that the differences could be due solely to errors in AUSGeoid98. As such, it is premature to assert that

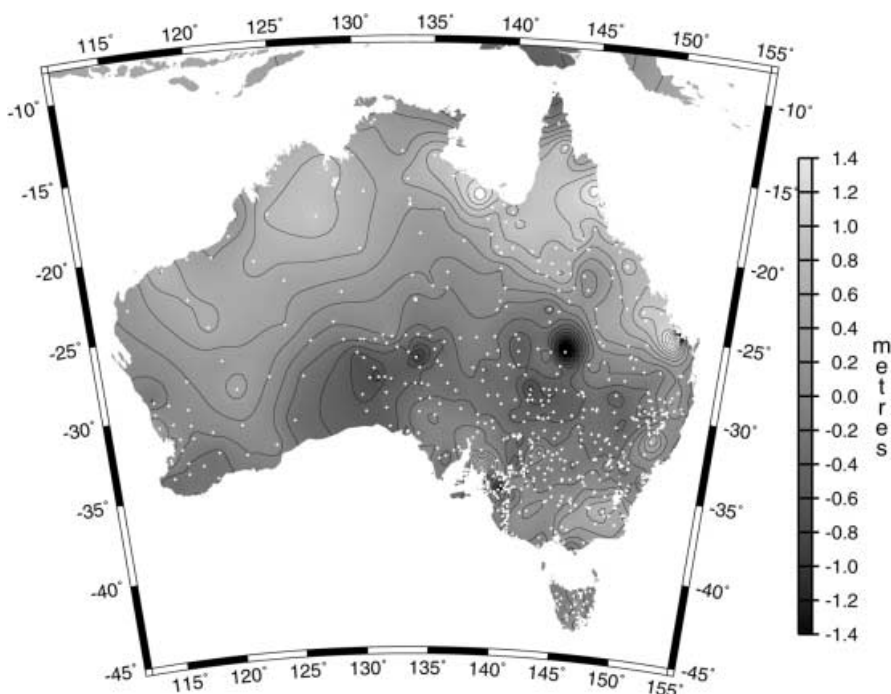


**Fig. 6.** Contours of the absolute differences between AUSGeoid98 and 1013 GPS–AHD data (Lambert conical projection)

AUSGeoid98 is able to unequivocally reveal the deficiencies in the AHD, although it does indicate the *possibility* of some region-dependent differences (Fig. 6).

Featherstone and Guo (submitted) also use least squares linear regression to determine if any significant trends exist in the differences between AUSGeoid98 and the 1013 GPS–AHD data as a function of AHD height, latitude or longitude (see Table 1). From Table 1, it can be seen that there are no significant trends evident between AUSGeoid98 and the GPS–AHD data as a function of AHD height or longitude. By way of comparison, the differences as a function of AHD height for AUSGeoid93, which omitted topographic corrections, show a significant dependency with elevation (gradient:  $0.020 \pm 0.005$  mm/m; correlation coefficient: 0.118). This alone indicates the use of topographic information in Australian geoid models, as is demanded by theory.

Table 1 also shows that there is a significant trend in the differences between AUSGeoid98 and the GPS–AHD data as a function of latitude, which equates to  $\sim 0.263$  mm/km. This could be attributed to either systematic north–south levelling errors (e.g. Bomford 1971, p. 241) or the larger north–south trend in sea-surface topography affecting the 32 tide gauge heights that were fixed to zero in the adjustments of the AHD (cf. Roelse et al. 1971), or to both. However, a north–south error in AUSGeoid98 cannot be ruled out as the sole explanation for this observation. Clearly, further work is required before Australian gravimetric geoid models can be used to unequivocally identify errors in the AHD.

## 6 Summary and conclusions

This paper has summarised all aspects involved in the computation of the new Australian geoid model, called AUSGeoid98. The interested reader is referred to the references cited herein for more detailed descriptions of the theories and techniques used. To summarise, the data used to compute AUSGeoid98 were taken from the EGM96 global geopotential model, the 1996 release of the Australian gravity data base, a 9 by 9 arc-second nationwide digital elevation model, and satellite–altimeter-derived marine gravity anomalies. Considerable effort was applied to the preparation of the gravity data, which included the reduction of the effects of unrepresentative sampling in the land gravity observations and the combination of ship-track and altimeter-derived marine gravity anomalies using least squares collocation, both of which improved the geoid solution. Gravimetric terrain corrections and their indirect effects

were computed for the first time in any Australian gravimetric geoid model.

A hybrid approach [Eq. (14)] of the generalised Stokes scheme with a deterministically modified kernel [Eq. (8)] and the remove–compute–restore technique was used to compute the residual geoid undulations from the residual gravity data based on EGM96. In order to allow computation of a 2 by 2 arc-minute geoid model in a reasonable timeframe, the 1-D-FFT technique was adapted to use a spherical cap of limited spatial extent ( $\psi_0 = 1^\circ$ ) together with a deterministically modified kernel for  $M = 20$ . These adaptations sequentially improved the gravimetric geoid solution over the use of the whole data area in conjunction with the spherical Stokes kernel [Eq. (16)], probably because of peculiarities in the Australian data.

Nationwide and regional comparisons of AUSGeoid98 with GPS–AHD data show some substantial improvements over its predecessor, AUSGeoid93. However, the RMS fit of AUSGeoid98, after geometrical estimation of the zero-degree term and other constant biases, to a nationwide set of 906 GPS–AHD control points is  $\pm 0.364$  m. This is worse than the fits presented for gravimetric geoid models in other parts of the world. An explanation for this is that the AHD is a third-order vertical datum that departs from the classical geoid by  $\sim 1$  m, which will contribute to a large proportion of this RMS value. However, errors in the

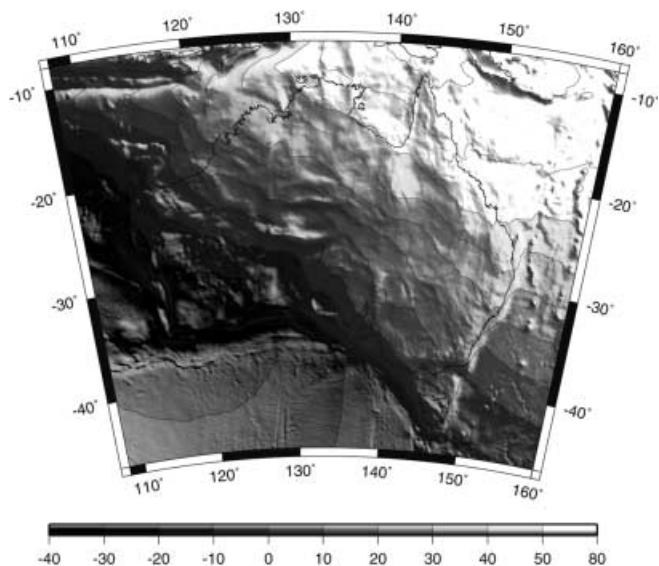


Fig. 7. The AUSGeoid98 geoid model of Australia (contours in metres with respect to GRS80; Lambert conical projection) illumination from the north-east

**Table 1.** Regression and correlation coefficients of the absolute differences between 1013 GPS–AHD data and AUSGeoid98 as a function of AHD height, latitude and longitude

Parameter	Gradient	Intercept	Correlation coefficient
AHD height	$0.005 \pm 0.003$ mm/m	$-0.0155 \pm 0.0133$ m	0.048
Latitude	$0.0292 \pm 0.0014$ m/arc-degree	$0.9153 \pm 0.0455$ m	0.542
Longitude	$-0.0007 \pm 0.0009$ m/arc-degree	$0.0911 \pm 0.1285$ m	-0.023

gravimetric geoid due to the quality of the Australian gravity data and the computational techniques used cannot be ruled out. Therefore, further research is required to refine both the Australian gravimetric geoid model and the definition and realisation of the AHD.

## 7 Postscript

AUSGeoid98 geoid heights with respect to the GRS80 ellipsoid (Fig. 7), deflections of the vertical at the geoid with respect to GRS80, estimated from the north–south and east–west gradients of AUSGeoid98, and Windows-based interpolation software can be downloaded, free of charge, from AUSLIG's web site (<http://www.auslig.gov.au/geodesy/ausgeoid/geoid.htm>). Alternatively, AUSGeoid98 values can be bi-cubically interpolated from the 2 by 2 arc-minute grid using an on-line facility at the same web site.

*Acknowledgements.* We would like to thank the following individuals for their many and varied contributions throughout the AUSGeoid98 project: Jon Evans, Matt Higgins, Simon Holmes, Joe Olliver, Merrin Pearse, Petr Vanicek and Kefei Zhang. We gratefully acknowledge the following organisations for their supply of data: the AGSO, AUSLIG, NASA, NIMA, GSFC, Scripps, and the surveying agencies of the state and territory governments of Australia. Without the kind supply of data, most of the AUSGeoid98 project would not have been possible. Thanks also go to the three reviewers (Dennis Milbert, Richard Rapp and Jian cheng Li) for their very constructive critiques of an earlier version of this manuscript. The research that led to AUSGeoid98 was supported financially by ARC large grant A49331318 to Will Featherstone, Bill Kearsley and John Gilliland. We also acknowledge continued funding for our Australian gravity field research through ARC large grant A39938040.

## References

- Bomford G (1971) *Geodesy*, 3rd edn. Oxford University Press, Oxford
- Carroll D, Morse MP (1996) A national digital elevation model for resource and environmental management. *Cartography* 25: 395–405
- Evans JD, Featherstone WE (2000) Improved convergence rates for the truncation error in geoid determination. *J Geod* 74: 239–248
- Featherstone WE (1995) On the use of Australian geodetic datums in gravity field determination. *Geom Res Aust* 62: 17–36
- Featherstone WE (1998) Do we need a gravimetric geoid or a model of the base of the Australian Height Datum to transform GPS heights? *Aust Surv* 43: 273–280
- Featherstone WE (1999) Tests of two forms of Stokes's integral using a synthetic gravity field based on spherical harmonics. In: Krumm F, Schwarze VS (eds) *Quo Vadis Geodesia?* University of Stuttgart, Stuttgart, pp 101–112
- Featherstone WE (2000) Refinement of a gravimetric geoid using GPS and levelling data. *J Surv Eng* 126: 27–56
- Featherstone WE, Guo W (submitted) Spatial evaluations of the precision of AUSGeoid98 and AUSGeoid93 using GPS and AHD data. *Geom Res Aust*
- Featherstone WE, Kirby JF (2000) The reduction of aliasing in gravity anomalies and geoid heights using digital terrain data. *Geophys J Int* 141: 2004–2012
- Featherstone WE, Sideris MG (1998) Modified kernels in spectral geoid determination: first results from Western Australia. In: Forsberg R, Feissl M, Dietrich R (eds) *Geodesy on the move*. Springer, Berlin Heidelberg New York, pp 188–193
- Featherstone WE, Evans JD, Olliver JG (1998) A Meissl-modified Vanicek and Kleusberg kernel to reduce the truncation error in gravimetric geoid computations. *J Geod* 72: 154–160
- Featherstone WE, Kearsley AHW, Gilliland JR (1997a) Data preparations for a new Australian gravimetric geoid. *Aust Surv* 42: 33–44
- Featherstone WE, Kirby JF, Zhang KF, Kearsley AHW, Gilliland JR (1997b) The quest for a new Australian gravimetric geoid. In: Segawa J, Fujimoto H, Okubo S (eds) *Gravity, geoid and marine geodesy*. Springer, Berlin Heidelberg New York, pp 581–588
- Fei ZL, Sideris MG (2000) A new method for computing the ellipsoidal correction for Stokes's formula. *J Geod* 74: 223–231
- Fisher I, Slutsky M (1967) A preliminary geoid chart of Australia. *Aust Surv* 21: 327–332
- Forsberg R (1990) A new high-resolution geoid of the Nordic area. In: Rapp RH, Sanso F (eds) *Determination of the geoid*. Springer, Berlin Heidelberg New York, pp 241–250
- Forsberg R (1998) The use of spectral techniques in gravity field modelling: trends and perspectives. *Phys Chem Earth* 23: 31–39
- Forsberg R, Featherstone WE (1998) Geoids and cap sizes. In: Forsberg R, Feissl M, Dietrich R (eds) *Geodesy on the move*. Springer, Berlin Heidelberg New York, pp 194–200
- Forsberg R, Sideris MG (1993) Geoid computations by the multi-band spherical FFT approach. *Bull Géod* 18: 82–90
- Fraser AR, Moss FJ, Turpie A (1976) Reconnaissance gravity survey of Australia. *Geophysics* 41: 1337–1345
- Freund KA, Steed J, Kearsley AHW (1997) A geoid for the Australian Capital Territory. *Aust Surv* 42: 25–32
- Fryer JG (1972) The Australian geoid. *Aust Surv* 24: 203–214
- Gachari MK, Olliver JG (1998) A high-resolution gravimetric geoid of East Africa. *Surv Rev* 34(269): 421–436
- Gilliland JR (1987) An Australian gravity anomaly data bank for geoid calculations. *Aust Surv* 33: 578–581
- Gilliland JR (1989) A gravimetric geoid of Australia. *Aust Surv* 34: 699–706
- Grushinsky NP, Sazhina NB (1971) The gravitational field and the geoid of Australia. *J Geol Soc Aust* 18: 183–199
- Haagmans RRN, de Min E, van Gelderen M (1993) Fast evaluation of convolution integrals on the sphere using 1D-FFT, and a comparison with existing methods for Stokes's integral. *Manuscr Geod* 18: 227–241
- Heiskanen WH, Moritz H (1967) *Physical geodesy*, Freeman, San Francisco
- Huang J, Vanicek P, Novak P (2000) An alternative algorithm to FFT for the numerical evaluation of Stokes's integral. *Stud Geophys Geod* 44: 374–380
- Hutchinson MF (1989) A new procedure for gridding elevation and streamline data with automatic removal of spurious points. *J Hydrol* 106: 211–232
- Inter-governmental Committee on Surveying Mapping (1996) *Standards and specifications for control surveys*. Sp publ no. 1, Inter-governmental Committee on Surveying and Mapping, Canberra, Australia
- Johnston GM, Featherstone WE (1998a) AUSGeoid98 computation and validation: exposing the hidden dimension. *Proc 39th Aust Surv Cong*, Launceston, Australia. pp 105–116
- Johnston GM, Featherstone WE (1998b) AUSGeoid98: a new gravimetric geoid for Australia. *Proc Inst Eng Mining Surv Aust 24th Conf*, Alice Springs, Australia
- Kearsley AHW (1988a) Tests on the recovery of precise geoid height differences from gravimetry. *J Geophys Res* 93(B6): 6559–6570
- Kearsley AHW (1988b) The determination of the geoid–ellipsoid separation for GPS levelling. *Aust Surv* 34: 11–18
- Kearsley AHW, Govind R (1992) The geoid in Australia: a status report. *Aust Surv* 36: 30–40
- Kearsley AHW, Steed J (1995) AUSGeoid93. *Int Geoid Serv Bull* 2: 1–6

- Kirby JF, Featherstone WE (1997) A study of zero- and first-degree terms in geopotential models over Australia. *Geom Res Aust* 66: 93–108
- Kirby JF, Featherstone WE (1999) Terrain correcting Australian gravity observations using the national digital elevation model and the fast Fourier transform. *Aust J Earth Sci* 46: 555–562
- Kirby JF, Forsberg R (1998) A comparison of techniques for the integration of satellite altimeter and surface gravity data for geoid determination. In: Forsberg R, Feissel M, Deitrich R (eds) *Geodesy on the move*. Springer, Berlin Heidelberg New York, pp 207–212
- Kirby JF, Featherstone WE, Kearsley AHW (1998) Tests of the DMA/GSFC geopotential models over Australia. *Int Geoid Serv Bull* 7: 2–13
- Knudsen P, Andersen OB (1998) Global marine gravity and mean sea surface from multi-mission satellite altimetry. In: Forsberg R, Feissel M, Deitrich R (eds) *Geodesy on the move*. Springer, Berlin Heidelberg New York, pp 132–137
- Lemoine FG, Kenyon SC, Factor JK, Trimmer RG, Pavlis NK, Chinn DS, Cox CM, Klosko SM, Luthcke SB, Torrence MH, Wang YM, Williamson RG, Pavlis EC, Rapp RH, Olson TR (1998) The development of the joint NASA GSFC and the National Imagery and Mapping Agency (NIMA) geopotential model EGM96. NASA/TP-1998-206861, National Aeronautics and Space Administration, Maryland, USA
- Lines JD (1992) Australia on paper – the story of Australian mapping. Fortune Publications, Box Hill, Australia
- Martinec Z, Vaníček P (1994a) Indirect effect of topography in the Stokes–Helmert technique for a spherical approximation of the geoid. *manusc geod* 19: 213–219
- Martinec Z, Vaníček P (1994b) Direct topographical effect of Helmert's condensation for a spherical approximation of the geoid. *manusc geod* 19: 257–268
- Martinec Z, Vaníček P (1997) Formulation of the boundary-value problem for geoid determination with a higher-degree reference field. *Geophys J Int* 126: 219–228
- Martinec Z, Vaníček P, Mainville A, Veronneau M (1996) Evaluation of topographical effects in precise geoid computation from densely sampled heights. *J Geod* 70: 746–754
- Mather RS (1969) The free-air geoid of Australia. *Geophys J Roy Astron Soc* 18: 499–516
- Morelli C, Gantar C, Honkaslo T, McConnel RK, Tanner TG, Szabo B, Uotila U, Whalen CT (1971) The International Gravity Standardisation Network (IGSN71). *Bull Géod*, sp publ 4
- Moritz H (1968) On the use of the terrain correction in solving Molodensky's problem. Rep 108, Department of Geodetic Science and Surveying, The Ohio State University, Columbus
- National Mapping Council (1986) Australian geodetic datum technical manual, National Mapping Council, Canberra, Australia, 62 pp
- Paul MK (1973) A method of evaluating the truncation error coefficients for geoidal height. *Bull Géod* 47: 413–425
- Rapp RH (1994) Separation between reference surfaces of selected vertical datums. *Bull Géod* 69: 26–31
- Rapp RH, Pavlis NK (1990) The development and analysis of geopotential coefficient models to spherical harmonic degree 360: OSU89A and OSU89B. *J Geophys Res* 95(B13): 21 855–21 911
- Rapp RH, Wang YM, Pavlis NK (1991) The Ohio State 1991 geopotential and sea surface topography harmonic coefficient model. Rep 410, Department of Geodetic Science and Surveying, The Ohio State University, Columbus, USA
- Roelse A, Granger HW, Graham JW (1971) The adjustment of the Australian levelling survey 1970–71. Report 12, Division of National Mapping, Canberra, Australia
- Sandwell DT, Smith WHF (1997) Marine gravity anomaly from Geosat and ERS 1 satellite altimetry. *J Geophys Res* 102(B5): 10 039–10 054
- Schwarz K-P, Sideris MG, Forsberg R (1990) The use of FFT techniques in physical geodesy. *Geophys J Int* 100: 485–514
- Sideris MG (1994) Geoid determination by FFT techniques. Lecture Notes, International School for the Determination and Use of the Geoid, DIIAR, Politecnico di Milano, Milan, Italy
- Sideris MG, Li YC (1993) Gravity field convolutions without windowing and edge effects. *Bull Géod* 67: 108–118
- Sideris MG, She BB (1995) A new, high-resolution geoid for Canada and part of the US by the 1D-FFT method. *Bull Géod* 69: 92–108
- Sjöberg LE, Hunegnaw A (2000) Some modifications of Stokes's formula that account for truncation and potential coefficient errors. *J Geod* 74: 232–238
- Smith DA, Milbert DG (1999) The GEOID96 high-resolution geoid height model for the United States. *J Geod* 73: 219–236
- Smith WHF, Wessel P (1990) Gridding with continuous curvature splines in tension. *Geophysics* 55: 293–305
- Steed J, Holtznagel S (1994) AHD heights from GPS using AUS-Geoid93. *Aust Surv* 39(1): 21–27
- Stewart MP (1998) How accurate is the Australian National GPS Network as a framework for GPS heighting? *Aust Surv* 43: 53–61
- Tscherning CC, Forsberg R, Knudsen P (1992) The GRAVSOFT package for geoid determination. In: Holota P, Vermeer M (eds) *Proc 1st IAG Continental Workshop of the Geoid in Europe*, Prague, pp 327–334
- Tziavos IN (1996) Comparisons of spectral techniques for geoid computations over large regions. *J Geod* 70(6): 357–373
- Vaníček P, Featherstone WE (1998) Performance of three types of Stokes's kernel in the combined solution for the geoid. *J Geod* 72: 684–697
- Vaníček P, Kleusberg A (1987) The Canadian geoid – Stokesian approach. *manusc geod* 12: 86–98
- Vaníček P, Martinec Z (1994) The Stokes–Helmert scheme for the evaluation of a precise geoid. *Manusc Geod* 19: 119–128
- Vaníček P, Sjöberg LE (1991) Reformulation of Stokes's theory for higher than second-degree reference field and modification of integration kernels. *J Geophys Res* 96(B4): 6529–6540
- Vaníček P, Huang JL, Novak P, Pagiatakis SD, Veronneau M, Martinec Z, Featherstone WE (1999) Determination of the boundary values for the Stokes–Helmert problem. *J Geod* 73: 180–192
- Vaníček P, Kleusberg A, Martinec Z, Sun W, Ong P, Najafi M, Vajda P, Harrie L, Tomasek P, ter Horst B (1995) Compilation of a precise regional geoid. Rep for Geodetic Survey Division, Geomatics Sector, Natural Resources Canada, Ottawa
- Vincent S, Marsh JG (1973) Global detailed gravimetric geoid. In: Vies G (ed) *Proc Int Symp on the Use of Artificial Earth Satellites for Geodesy and Geodynamics*, Athens, pp 825–855
- Wellman P, Barlow BC, Murray AS (1985) Gravity base station network values. Rep 261, Australian Geological Survey Organisation, Canberra
- Wessel P, Watts AB (1988) On the accuracy of marine gravity measurements. *J Geophys Res* 94(B4): 7685–7729
- Wichiencharoen C (1982) The indirect effects on the computation of geoid undulations. Rep 336, Department of Geodetic Science, The Ohio State University, Columbus, USA
- Zhang KF (1997) An evaluation of FFT geoid determination techniques and their application to Australian GPS heighting. Ph.D. thesis, School of Surveying and Land Information, Curtin University of Technology, Perth, Australia